applied sciences

Article

Physical Simulation of the Spectrum of Possible Electromagnetic Effects of Upward Streamer Discharges on Model Elements of Transmission Line Monitoring Systems Using Artificial Thunderstorm Cell

Nikolay Lysov *, Alexander Temnikov, Leonid Chernensky, Alexander Orlov, Olga Belova, Tatiana Kivshar, Dmitry Kovalev and Vadim Voevodin

Department of Electrophysics and High Voltage Technique, Moscow Power Engineering Institute, National Research University, 111250 Moscow, Russia; TemnikovAG@mpei.ru (A.T.); ChernenskyLL@mpei.ru (L.C.); orlovav@mpei.ru (A.O.); belovaos@mail.ru (O.B.); geratk@mail.ru (T.K.); kovalevdi@list.ru (D.K.); voevodinvv@mpei.ru (V.V.)
* Correspondence: streamer.corona@gmail.com; Tel.: +7-9168456253

Featured Application: The results of this work can be used to assess the reliability of electric power facilities' monitoring systems during thunderstorms. In addition to direct lightning strikes, the correct operation of monitoring systems can also be influenced by incomplete upward discharges, including those from nearby objects.

check for updates

Citation: Lysov, N.; Temnikov, A.; Chernensky, L.; Orlov, A.; Belova, O.; Kivshar, T.; Kovalev, D.; Voevodin, V. Physical Simulation of the Spectrum of Possible Electromagnetic Effects of Upward Streamer Discharges on Model Elements of Transmission Line Monitoring Systems Using Artificial Thunderstorm Cell. *Appl. Sci.* **2021**, *11*, 8723. https://doi.org/10.3390/app11188723

Academic Editors: Massimo Brignone and Daniele Mestriner

Received: 9 August 2021
Accepted: 14 September 2021
Published: 18 September 2021

Abstract: The results of a physical simulation using negatively charged artificial thunderstorm cells to test the spectrum of possible electromagnetic effects of upward streamer discharges on the model elements of transmission line monitoring systems (sensor or antennas) are presented. Rod and elongated model elements with different electric field amplification coefficients are investigated. A generalization is made about the parameters of upward streamer current impulse and its electromagnetic effect on both kinds of model elements. A wavelet analysis of the upward streamer corona current impulse and of the signal simultaneously induced in the neighboring model element is conducted. A generalization of the spectral characteristics of the upward streamer current and of the signals induced by the electromagnetic radiation of the nearby impulse streamer corona on model elements is made. The reasons for super-high and ultra-high frequency ranges in the wavelet spectrum of the induced electromagnetic effect are discussed. The characteristic spectral ranges of the possible electromagnetic effect of upward streamer flash on the elements of transmission line monitoring systems are considered.

Keywords: artificial thunderstorm cell; lightning; upward streamer discharges; electromagnetic radiation spectrum; wavelet; transmission line monitoring system; model element; simulation

1. Introduction

Software, computing complexes, and artificial intelligence algorithms are being increasingly introduced into power management systems, and include various remote monitoring systems for transmission lines. These systems use collected data to form control signals that make operational decisions [1–7]. At the same time, functional problems continue to appear during the use of digital technology and computing systems in the online monitoring of the air transmission lines (e.g., sensors of various kinds, analog–digital converters for the processing of recorded signals, and antenna and receiver-transmitting devices of different shapes and sizes [6–10]) under the influence of thunderclouds and lightning. Most often, these devices are rods, cylindrical, or flat. It is therefore necessary to ensure their electromagnetic compatibility [11–13]. Moreover, it is not entirely clear how these devices are affected by the different kinds of discharge phenomena that form on various design features of monitoring systems and/or the transmission lines while under the influence of thunderclouds and lightning (e.g., flashes of avalanche and streamer corona, ascending and downward leaders, the main discharge), or how the electromagnetic radiation they create will affect their functionality [12,14,15].

Those impacts are particularly dangerous, as they have frequencies close to the working frequencies of various elements and devices of the artificial intelligence system; this could be from hundreds of hertz to several gigahertz [6,8,12]. Sensors, receivers, communication systems, and in some cases, parts of the software-computing control complex of the transmission line monitoring system may be situated directly in the electric field area of thunderclouds and lightning discharge. In this case, exposure to electromagnetic radiation can occur in a wide frequency range, leading to interference, failures, distortions, false positives, and, accordingly, the disruption of normal functionality. Moreover, even the successful triggering of external lightning protection does not eliminate the possibility of an electrical objects' failure; this is a consequence of the impact of electromagnetic radiation of close lightning discharges in various frequency ranges at the different stages of its formation [14].

It is necessary to achieve a correct interpretation of the spectral characteristics of the electromagnetic radiation that affects the elements of the transmission line monitoring systems in the near field, and to determine their connection with the peculiarities of the formation of the lightning discharge between the thundercloud and the ground [16]. This requires investigation into the connection between the characteristic frequencies of the measured signal and the discharge processes taking place in the thundercloud; this must be conducted on objects on the surface of the earth and under a thundercloud, and between the thundercloud and the ground during the formation of lightning discharge [16–20].

The use of artificial thunderstorm cells of negative polarity makes it possible to physically simulate and investigate the characteristics of various types of electrical discharges and the electromagnetic radiation they create. This can be formed on the model elements of the monitoring systems of transmission lines, or be imposed on them during close lightning strikes. The purpose of this work is to physically model (using artificial thunderstorm cells) the spectrum of the possible direct and induced electromagnetic impact of upward streamer discharges in order to determine their influence on the functionality of the intelligent systems that monitor the air transmission lines. These discharges may form on the transmission line intelligent monitoring systems (receiving-transmission devices of different kinds), as well as on the adjacent, grounded structures of the transmission line.

2. Experimental Schemes

This research was performed using equipment from the core shared research facilities, namely the high-voltage research complex of the National Research University, the Moscow Power Engineering Institute, which allows the creation of artificial storm cells of negative polarity with a potential of up to 1.5 MV [21]. As a result, a strong electric field appears in the gap between the artificial thunderstorm cell of negative polarity and the grounded plane, which develops all the forms of spark discharge that are characteristic of a thunderstorm, including the leader and main stage.

The measuring units of monitoring systems are usually located on transmission towers and phase wires. The measuring unit includes sensors for measuring main parameters, a processor module, and a data transmission system. Depending on their functional purpose, monitoring systems can use various types of sensors and transmitters (transceivers) of a rod or elongated type with sizes ranging from several centimeters to tens of centimeters. Sensors can have an almost spherical or cylindrical shape, or have a complex shape with protruding rod elements [5,6,8]. Since the structural elements of the transmission tower, as well as the phase and grounded wires, are also close in shape to a rod or cylindrical form, the following two experimental schemes with rod or cylindrical electrodes were chosen for the physical modeling used during the research.

Two experimental schemes were used for a physical simulation of the spectrum. The first scheme simulated upward streamer discharges formed from the rod sensors (or antenna devices) or the effects of the electromagnetic radiation of the upward streamer discharges, formed on the rod elements of the transmission line design on the nearby model sensors (Figure 1). The second scheme simulated the analogous situation, but for the case of sensors (or antenna devices) of the cylinder type and of limited length, and the phase and ground wires (Figure 2). The distance between two grounded electrodes (one simulating the element from which an ascending streamer discharge is formed, and the other simulating the element on which the signal is induced by this discharge) was in the range of 15 to 30 cm. In the simulation, a monitoring system element and the places of formation of ascending streamer discharges on an overhead power transmission line were situated relatively close together.

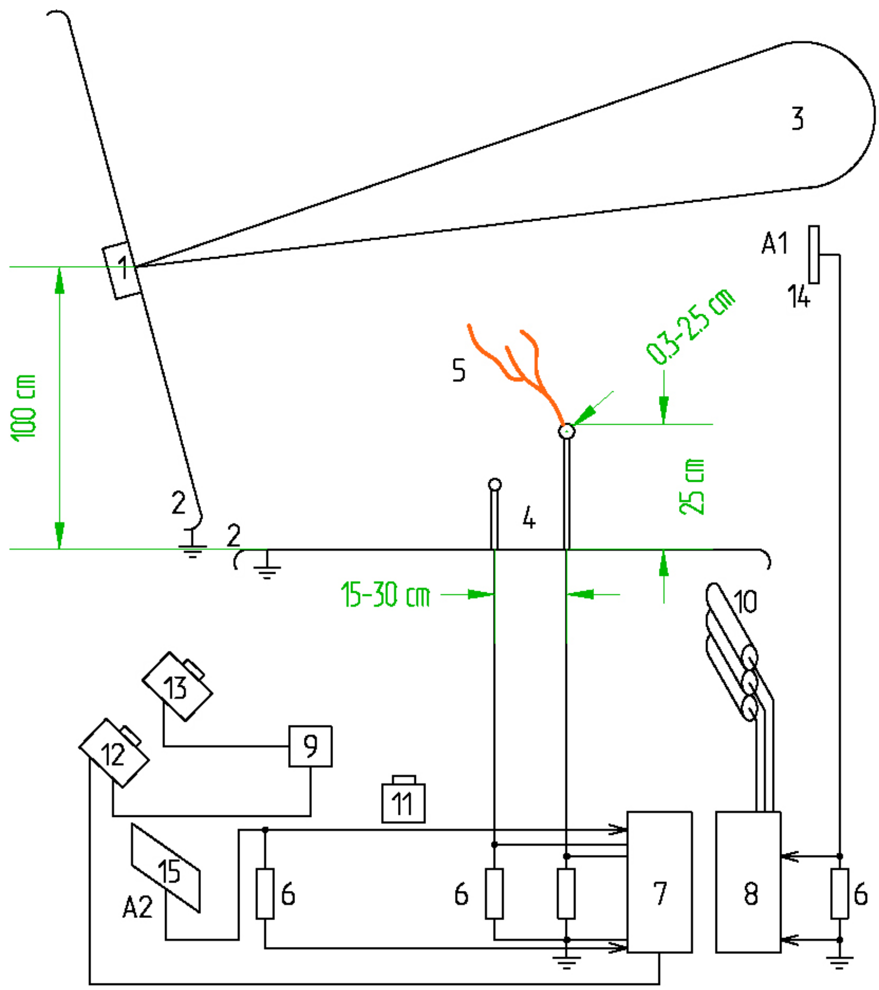

Figure 1. First scheme of experimental and measurement setup: 1—charged aerosol generator; 2—grounded electrostatic screens; 3—artificial thunderstorm cell; 4—rod electrodes; 5—upward streamer discharge; 6—shunts; 7,8—digital oscilloscope; 9—trigger generator; 10—system of photomultipliers; 11—digital photo camera; 12—photomultiplier; 13—CCD-camera; 14, 15—flat antennas.

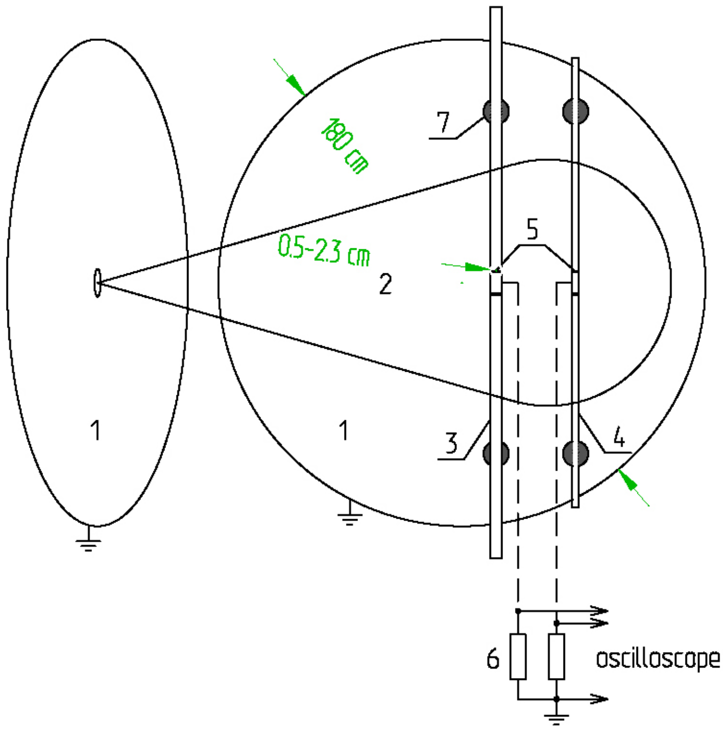

Figure 2. Second scheme of experimental and measurement setup: 1—grounded electrostatic screens; 2—artificial thunderstorm cell; 3,4—cylinder electrodes; 5—isolated elongated elements; 6—shunts: 7—insulators.

The conditions for the formation (the occurrence and subsequent development) of ascending streamer discharges originating from the grounded elements of monitoring systems in an external electric field created by a thundercloud and/or a descending lightning leader significantly depend on the nature of the distribution of the local electric field in the area near them [22]. Therefore, when conducting experimental studies, the radii of the vertices of rod model objects and the radii of model cylindrical objects varied in range from 0.3 to 2.5 cm for rod elements, and from 0.5 to 2.3 cm for extended elements. The height of the electrodes varied from 15 to 37 cm. Model rod electrodes were made of brass or aluminum; model cylindrical electrodes (tubes) were made of brass, aluminum, or steel. Elements of sensors, transmission towers, and phase and grounded wires were also made of these materials. As a result, the experiment simulated the formation of ascending discharge phenomena from elements of cyber-physical objects and systems with significantly different electric field amplification coefficients under the influence of atmospheric electricity and lightning. To analyze the influence this factor had on the experimental results, all model elements were divided into three groups according to the electric field amplification coefficient: group I had an amplification coefficient < 10; group II had an amplification coefficient < 25; group III had an amplification coefficient > 25.

Examples of the formation of upward streamer discharges from the grounded rods and elongated model elements under the negative polarity artificial thunderstorm cell are shown in Figures 3 and 4, respectively.

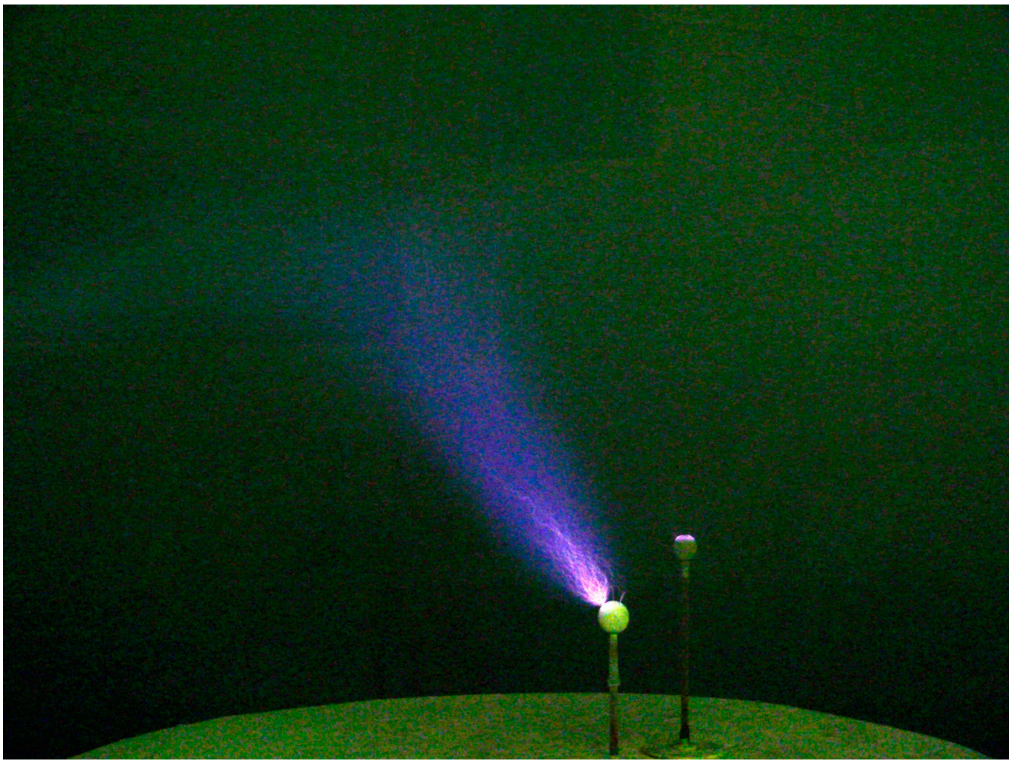

Figure 3. Upward streamer corona flash from the grounded rod model elements.

Figure 4. Upward streamer discharges from the grounded cylinder model element.

The characteristic oscillograms of the current impulse of powerful streamer corona flash and the corresponding induced electromagnetic effects (induced current) on the close rod or elongated model element are shown in Figure 5. The discharge current was registered using low-inductance shunts (6, Figures 1 and 2). The current induced by the discharge was registered using flat antennas (A1 and A2, Figure 1). Both signals were recorded by digital oscilloscopes Tektronix DPO7254 and Tektronix TDS3054C (Tektronix, Inc., Beaverton, OR, USA).

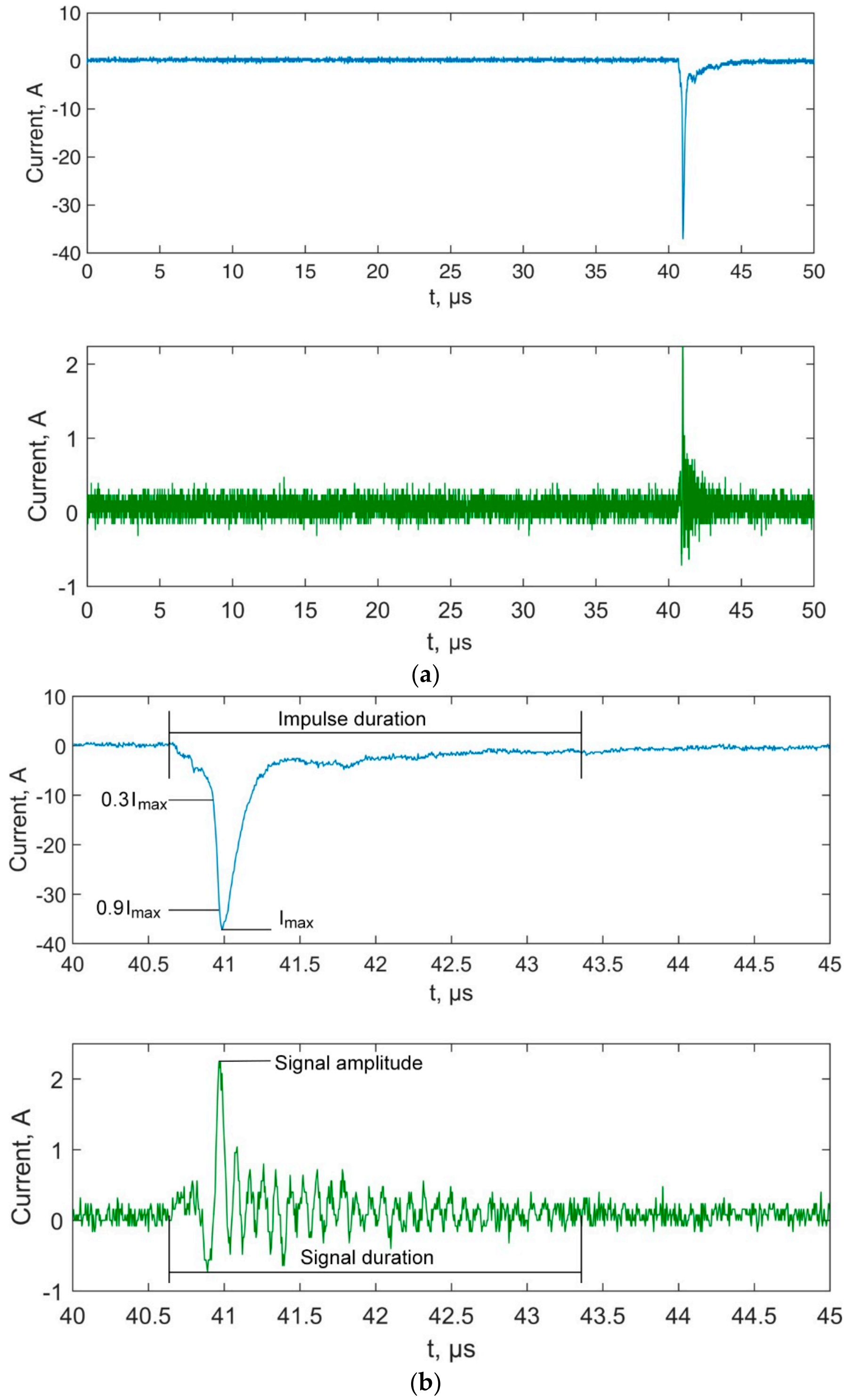

Figure 5. (**a**) Oscillograms of the upward streamer discharge current (upper) and induced electromagnetic effects (bottom). (**b**) Focused oscillograms of the formation of the upward streamer discharge current (upper) and induced electromagnetic effects (bottom).

For the impulse streamer corona flash of the upward discharge current amplitude, maximal current rise velocity, flowing charge, and impulse duration were determined. For induced electromagnetic effects on the signal amplitude of the nearby model elements, the duration of the induced signal was determined. The maximum value of the current pulse was described as the current amplitude (Imax). The time between the start and end of the impulse was described as the impulse duration. The start time of the pulse was decided based on the first time it crossed the zero value; similarly, the end time was decided based on the time of the first signal zero value following Imax. The maximal current rise velocity was specified as the ratio of the difference between 0.9 and 0.3 Imax of the signal duration between the points corresponding to 0.9 and 0.3 Imax (Figure 5b). The flowing charge was estimated by the integration of the current pulse from the pulse start time to the end time.

The spectral characteristics of the discharge current and the induced signals were determined based on a wavelet analysis, using the specially created program and the "Mexican Hat" wavelet [23,24]. In mathematics, a wavelet series is a representation of a square-integrable (real- or complex-valued) function by a certain orthonormal series generated by a wavelet. The fundamental idea behind wavelet transforms is that the transformation should only allow changes in the time extension, but not the shape. While the Fourier transform creates a representation of the signal in the frequency domain, the wavelet transform creates a representation of the signal in both the time and the frequency domain, thereby allowing efficient access to localized information about the signal. The upper level of the characteristic frequency, maximal intensity, and frequency of the maximal intensity in the wavelet spectrum was found. The characteristic wavelet spectrum for the currents and induced signal presented in Figure 5 are shown in Figures 6 and 7, respectively.

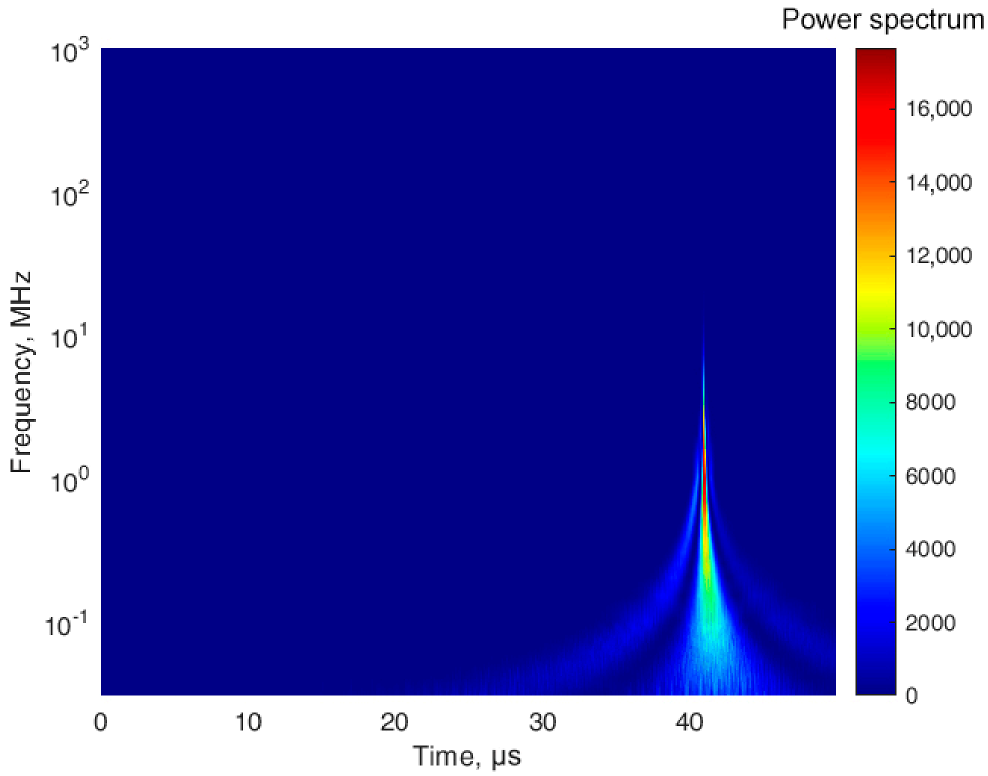

Figure 6. Wavelet spectrum of upward streamer corona current impulse.

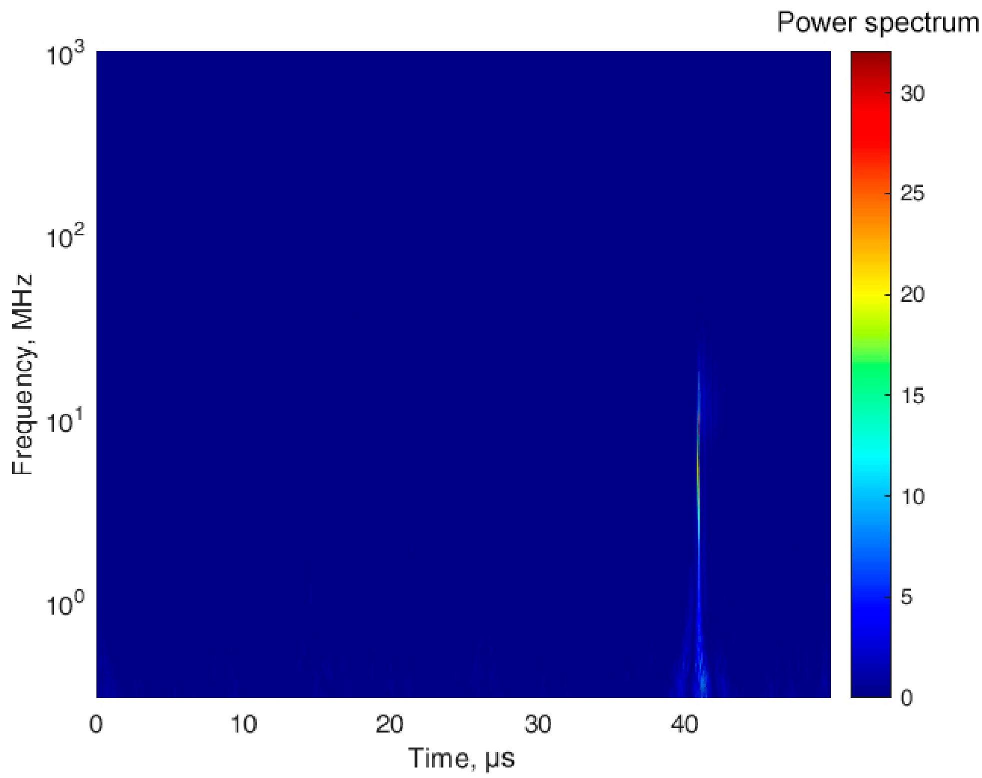

Figure 7. Wavelet spectrum of the signal induced in the nearby model element by the upward streamer corona flash.

3. Analysis of Results and Discussion

During the study, 530 experimental attempts were performed and processed, 222 of which were performed using the first experimental scheme, and 308 using the second.

The processed experimental results showed that the characteristics of the current pulse of the upward streamer corona with model rods and elongated elements depended on the characteristics of the electric field (group of amplification coefficient) near such objects (Tables 1 and 2). The impulse current of the streamer flash from the model elements with relatively low amplification coefficients (group I) showed average higher current amplitudes and charges, and less impulse duration. However, higher values of the maximal current rise velocity were observed for the model elements with amplification coefficients ranging from 10 to 25 (group II). For all groups of model amplification coefficients, the duration of the current impulse and flowing charge was on average higher for elongated model elements than for rods.

Table 1. Characteristics of the current impulse of streamer corona on the rod model elements (average values).

Amplification Coefficient	Group I	Group II	Group III
Current amplitude, A	8.45	5.11	3.26
Maximal current rise velocity, A/ns	0.13	0.17	0.14
Impulse duration, μs	2.65	5.24	2.98
Flowing charge, μC	4.38	4.17	1.96

It should be noted that for all groups of model element amplification coefficients, the characteristics of the signals induced in the elongated model elements by the neighboring upward streamer corona flash showed higher values than those of the rod model elements (Table 3).

Table 2. Characteristics of the current impulse of streamer corona on the cylinder model elements (average values).

Amplification Coefficient	Group I	Group II	Group III
Current amplitude, A	8.89	3.04	2.19
Maximal current rise velocity, A/ns	0.10	0.13	0.12
Impulse duration, μs	4.12	7.08	9.23
Flowing charge, μC	6.54	5.09	4.12

Table 3. Characteristics of the signals induced with nearby impulse streamer corona on the model elements (average values).

Source of Effect	Streamer Corona (Rod Model Element)		Streamer Corona (Elongated Model Element)	
Amplification Coefficient	Signal Amplitude, A	Signal Duration, μs	Signal Amplitude, A	Signal Duration, μs
Group I	0.94	1.06	1.18	1.12
Group II	1.36	0.31	1.41	0.52
Group III	1.02	0.69	1.22	0.97

The wavelet analysis showed that the spectral characteristics (upper frequency and frequency corresponding to maximal intensity) of a current impulse of an upward streamer flash had average values 1.5–9.0 times higher for the case of the rod model elements than for elongated elements for all the groups of model amplification coefficients (Tables 4 and 5). In some cases, an upper frequency ranging from 500 MHz to 1 GHz appeared in the wavelet spectrum of the current impulse of the streamer corona from the rod model elements related to group III (a higher amplification coefficient).

Table 4. Spectral characteristics of the current impulse of streamer corona on the rod model elements (average values).

Amplification Coefficient	Group I	Group II	Group III
Upper level of the characteristic frequency, MHz	9.9	13.2	83.5
Frequency of the maximal intensity, MHz	0.9	1.1	5.8
Maximal intensity, A2	2300	900	450

Table 5. Spectral characteristics of the current impulse of streamer corona on the elongated model elements (average values).

Amplification Coefficient	Group I	Group II	Group III
Upper level of the characteristic frequency, MHz	6.8	5.2	9.5
Frequency of the maximal intensity, MHz	0.5	0.4	1.8
Maximal intensity, A2	3600	800	200

A generalization of the spectral characteristics of the signals induced by the electromagnetic radiation of the nearby impulse streamer corona flash on model elements of different types showed the close values of all frequency parameters inside every group of the electric amplification coefficient for rod and elongated model elements (Tables 6 and 7). The maximal values of the upper level of the characteristic frequency in the wavelet spectrum of the induced signal (the electromagnetic radiation of upward streamers was sometimes in the range of 1.0–1.5 GHz) were discovered in group II (an amplification coefficient of 10–25). Group III (amplification coefficient > 25) showed similar, but slightly lower, values.

Table 6. Spectral characteristics of the signals induced with nearby impulse streamer corona on the rod model elements (average values).

Amplification Coefficient	Group I	Group II	Group III
Upper level of the characteristic frequency, MHz	111	795	397
Frequency of the maximal intensity, MHz	10	76	27
Maximal intensity, A2	10	14	9

Table 7. Spectral characteristics of the signals induced with nearby impulse streamer corona on the elongated model elements (average values).

Amplification Coefficient	Group I	Group II	Group III
Upper level of the characteristic frequency, MHz	123	809	528
Frequency of the maximal intensity, MHz	8	68	18
Maximal intensity, A2	12	10	9

Presumably, such high frequencies appear in the spectrum of the electromagnetic radiation of the upward streamer discharges due to their development in a highly divergent electric field. This leads to the rapid rise in the discharge current. As seen in Tables 1 and 2, the maximal current rise velocity was observed on model elements from group II.

Thus, it is suggested that the formation of electromagnetic radiation of the corona discharge in an avalanche and streamer form is presumably one of the key mechanisms of the electromagnetic influence on the discharge phenomena in artificial and natural storm cells and clouds that are located in the vicinity of model elements of cyber-physical objects, and systems in the super-high and ultra-high frequency range [15,25–27]. According to [26], the electromagnetic radiation of avalanches formed from rods and long (cylindrical) electrodes and in the head of streamers in various large electric fields have an electromagnetic radiation that can be clearly expressed in the range of 4.0–5.0 MHz to 0.9–1.0 GHz, from 1.0–2.0 MHz to 0.5–0.6 GHz, and from 0.5–1.0 MHz to 8–10 GHz. Another source of such ultra-high electromagnetic radiation of the streamer flash, as proposed in [27], could be the result of the streamers colliding inside a streamer zone. Both of these electromagnetic radiation formation mechanisms correlate to the characteristic frequency ranges of the wavelet spectrums of signals, and are guided on model rods and long elements of the neighboring flash of the streamer corona; these develop from another model element belonging to group II and group III, containing large force-strength factors of the electric field. Electromagnetic radiation with frequencies exceeding 1 GHz during streamer flashes in the electric field of a cloud charged with water drops was registered in [28] as well.

The possible electromagnetic effects of upward streamer flash on elements of transmission line monitoring systems in the determined characteristic spectral ranges are speculated. If upward streamer discharges form on the sensors (especially the rod kind, and on those included in group III) of the monitoring system, frequencies that are in the spectrum of a current impulse (up to dozens or hundreds of megahertz) will be in the working frequency range of the sensor. This could lead to sensor failure, including errors in the digital processing of data by the analog–digital converters [11–13,29].

Similar failures may also be encountered when the electromagnetic radiation of streamer corona flash originates near the monitoring, diagnostic, and control systems that affect its elements (e.g., sensors). Failures may also occur if analog–digital converters with working frequencies from several hundred kilohertz to several gigahertz are used for subsequent digital processing of the measuring information [5,6,8,11]. The electromagnetic radiation of the streamer corona flash ranging from hundreds of megahertz to gigahertz could impact nearby receiving/transmitting devices, and result in disruption, distortion, or a loss in informational transmission [8,11,12].

4. Conclusions

Physical modeling (using an artificial thunderstorm cell) of the possible influence of upward streamer discharges from the rod or elongated model elements of a power transmission line monitoring systems on their operation in the electric field of a thunderstorm cloud and/or lightning produced many results. Firstly, upward streamer discharges that formed on the monitoring systems model elements (i.e., sensors, and receiving and transmitting devices) can affect the functioning of these systems due to the fact that in the spectrum of their currents, there are frequencies of up to tens of megahertz, which is close to the operating frequencies of power transmission line monitoring systems. Secondly, upward streamer discharges on the model elements of power transmission lines can also induce signals in the neighboring rod or elongated elements of the monitoring systems. These signals are dangerous for the monitoring systems' operation, since the discharge spectrum contains frequencies of tens to hundreds of megahertz (up to units of gigahertz).

It was found that the parameters of the current pulse of upward streamer discharges, the signals that they induce in the neighboring elements, and their spectral characteristics depend on the electric field distribution near the model rod or elongated element (electric field amplification factor). The highest frequencies in the spectrum of the current pulse of the streamer corona flash are typical for the model elements with a high electric field amplification coefficient of >25. The highest frequencies in the spectrum of the signal induced in the neighboring element by the upward streamer discharges are typical for model elements with an amplification coefficient of 10–25. Thus, both the frequency ranges in the spectrum of the current pulse of upward streamer discharges formed from the model elements of sensors and receiving-transmitting devices of the power transmission line monitoring system and the frequency ranges in the spectrum of signals induced by close upward streamer discharges on these elements may appear close to the operating frequency ranges of analog-to-digital converters of sensors and/or devices for transmitting data in monitoring systems. This can lead to failures in monitoring systems operation, false alarms, incorrect transmission of information, and, as a result, create significant risks for the functionality of these systems during thunderstorms.

Author Contributions: Project administration and methodology, A.T.; software, L.C. and O.B.; visualization, T.K.; investigation, A.O. and N.L.; writing—original draft preparation, V.V.; funding acquisition, D.K. All authors have read and agreed to the published version of the manuscript.

Funding: This study conducted by Moscow Power Engineering Institute was financially supported by the Ministry of Science and Higher Education of the Russian Federation (project No. FSWF-2020-0019).

Institutional Review Board Statement: Not applicable.

Informed Consent Statement: Not applicable.

Data Availability Statement: Not applicable.

Conflicts of Interest: The authors declare no conflict of interest.

References

1. Hu, Y.; Liu, K. *Inspection and Monitoring Technologies of Transmission Lines with Remote Sensing*; Academic Press: Cambridge, MA, USA, 2017.
2. Li, S.; Li, J. Condition monitoring and diagnosis of power equipment: Review and prospective. *High Volt.* **2017**, *2*, 82–91. [CrossRef]
3. Deng, C.-J. Challenges and Prospects of Power Transmission Line Intelligent Monitoring Technology. *Am. Res. J. Comput. Sci. Inf. Technol.* **2019**, *4*, 1–11.
4. Zhirui, L.; Shengsuo, N.; Nan, J. Current Status and Development Trend of AC Transmission Line Parameter Measurement. *Autom. Electr. Power Syst.* **2017**, *41*, 181–191.
5. Liu, Y.; Yin, H.; Wu, T. Transmission Line on-line Monitoring System Based on Ethernet and McWiLL. In Proceedings of the International Conference on Logistics Engineering, Management and Computer Science (LEMCS 2015), Shenyang, China, 26–28 June 2015; pp. 680–683.
6. Working Group on Monitoring & Rating of Subcommittee 15.11 on Overhead Lines. Real-Time Overhead Transmission-Line Monitoring for Dynamic Rating. *IEEE Trans. Power Deliv.* **2016**, *31*, 921–927. [CrossRef]

7. Xing, Z.; Cui, W.C.; Liu, R.; Zheng, Z. Design and Application of Transmission Line Intelligent Monitoring System. In Proceedings of the 2020 International Conference on Energy, Environment and Bioengineering (ICEEB 2020), Xi'an, China, 7–9 August 2020; Volume 185. [CrossRef]
8. McCall, J.C.; Spillane, P.; Lindsey, K. Determining Crossing Conductor Clearance Using Line-Mounted LiDAR. In Proceedings of the CIGRE US National Committee 2015 Grid of the Future Symposium, Paris, France, 12 October 2015.
9. Wydra, M.; Kubaczynski, P.; Mazur, K.; Ksiezopolski, B. Time-Aware Monitoring of Overhead Transmission Line Sag and Temperature with LoRa Communication. *Energies* **2019**, *12*, 505. [CrossRef]
10. Chen, H.; Qian, Z.; Liu, C.; Wu, J.; Li, W.; He, X. Time-Multiplexed Self-Powered Wireless Current Sensor for Power Transmission Lines. *Energies* **2021**, *14*, 1561. [CrossRef]
11. Hoole, P.R.P.; Sharip, M.R.M.; Fisher, J.; Pirapaharan, K.; Othman, A.K.H.; Julai, N.; Rufus, S.A.; Sahrani, S.; Hoole, S.R.H. Lightning Protection of Aircraft, Power Systems and Houses Containing IT Network Electronics. *J. Telecommun. Electron. Comput. Eng.* **2017**, *9*, 3–10.
12. Ahmad, M.R.; Esa, M.R.M.; Cooray, V.; Dutkiewicz, E. Interference from cloud-to-ground and cloud flashes in wireless communication system. *Electr. Power Syst. Res.* **2014**, *113*, 237–246. [CrossRef]
13. Borisov, R.K.; Zhulikov, S.S.; Koshelev, M.A.; Maksimov, B.K.; Mirzabekyan, G.Z.; Turchaninova, Y.S.; Khrenov, S.I. A Computer-aided design system for protecting substations and overhead power lines from lightning. *Russ. Electr. Eng.* **2019**, *90*, 86–91. [CrossRef]
14. Cooray, V. *Lightning Electromagnetics*; IET Publishing: London, UK, 2012.
15. Cooray, V.; Cooray, G. Electromagnetic fields of accelerating charges: Applications in lightning protection. *Electr. Power Syst. Res.* **2017**, *145*, 234–247. [CrossRef]
16. Nag, A.; Murphy, M.J.; Schulz, W.; Cummins, K.L. Lightning location systems: Insights on characteristics and validation technique. *Earth Space Sci.* **2015**, *2*, 65–93. [CrossRef]
17. Chen, M.; Du, Y.; Burnett, J.; Dong, W. The electromagnetic radiation from lightning in the interval of 10 kHz to 100 MHz. In Proceedings of the 12th International Conference on Atmospheric Electricity, Versailles, France, 9–14 June 2003.
18. Makela, J. *Electromagnetic Signatures of Lightning near the HF Frequency Band*; Finnish Meteorological Institute: Helsinki, Finland, 2009.
19. Dong, W.; Liu, H. Observation of compact intracloud discharges using VHF broadband interferometer. In Proceedings of the 2012 International Conference on Lightning Protection (ICLP), Vienna, Austria, 2–7 September 2012.
20. Rakov, V.A. Electromagnetic Methods of Lightning Detection. *Surv. Geophys.* **2013**, *34*, 731–753. [CrossRef]
21. Temnikov, A.G. Using of artificial clouds of charged water aerosol for investigations of physics of lightning and lightning protection. In Proceedings of the 2012 International Conference on Lightning Protection (ICLP), Vienna, Austria, 2–7 September 2012. [CrossRef]
22. Bazelyan, E.M.; Raizer, Y.P. *Lightning Physics and Lightning Protection*; IoP Publishing: Bristol, UK; New York, NY, USA, 2000.
23. Esa, M.R.M.; Ahmad, M.R.; Cooray, V. Wavelet analysis of the first electric field pulse of lightning flashes in Sweden. *J. Atmos. Res.* **2014**, *138*, 253–267. [CrossRef]
24. Temnikov, A.G.; Chernensky, L.L.; Belova, O.S.; Orlov, A.V.; Zimin, A.S. Spectral characteristics of discharges from artificial charged aerosol cloud. In Proceedings of the 2014 International Conference on Lightning Protection (ICLP), Shanghai, China, 11–18 October 2014.
25. Cooray, V.; Cooray, G. The Electromagnetic Fields of an Accelerating Charge: Applications in Lightning Return-Stroke Models. *IEEE Trans. Electromagn. Compat.* **2010**, *52*, 944–955. [CrossRef]
26. Cooray, V.V.; Cooray, G. Electromagnetic radiation field of an electron avalanche. *Atmos. Res.* **2012**, *117*, 18–27. [CrossRef]
27. Shi, F.; Liu, N.; Dwyer, J.R.; Ihaddadene, K.M.A. VHF and UHF electromagnetic radiation produced by streamers in lightning. *Geophys. Res. Lett.* **2019**, *46*, 443–451. [CrossRef]
28. Gushchin, M.E.; Korobkov, S.V.; Zudin, I.Y.; Nikolenko, A.S.; Mikryukov, P.A.; Syssoev, V.S.; Sukharevsky, D.I.; Orlov, A.I.; Naumova, M.Y.; Kuznetsov, Y.A.; et al. Nanosecond electromagnetic pulses generated by electric discharges: Observation with clouds of charged water droplets and implications for lightning. *Geophys. Res. Lett.* **2021**, *48*, e2020GL092108. [CrossRef]
29. Judge, M.A.; Manzoor, A.; Ahmed, F.; Kazmi, S.; Khan, Z.A.; Qasim, U.; Javaid, N. Monitoring of Power Transmission Lines Through Wireless Sensor Networks in Smart Grid. In Proceedings of the 11th International Conference on Innovative Mobile and Internet Services in Ubiquitous Computing, Torino, Italy, 28–30 June 2017.